DEVELOPMENT OF THREE-DIMENSIONAL CLOTHING MODEL FOR A COMPUTER-SIMULATED PERSON INTEGRATED WITH A THERMOREGULATION MODEL

Sena Hyodo[1*], *Kei* Murota[1], *Sung-Jun* Yoo[2], and *Kazuhide* Ito[2]

[1]Interdisciplinary Graduate School of Engineering Sciences, Kyushu University, Japan
[2]Faculty of Engineering Sciences, Kyushu University, Japan

Abstract: In recent years, an integrated analysis of computational fluid dynamics (CFD) and computer simulation person (CSP), especially to reproduce the shape of the human body, has been conducted to estimate the interaction between the human body and its surrounding indoor environment. Meanwhile, clothing is often treated in a simplified manner, as a means of resistance to heat and pollutant transfer, and there is sufficient room for improvement in the hygrothermal and scalar transfer phenomena in and around clothing with a complex geometry. In this study, some garment models with complex geometry and others with simplified geometry were created with a CSP, and airflow, temperature, and humidity were investigated along with the CSP. It was assumed that only heat and water vapor were transported in the garment. As a result, the naked model was found to be over-or underestimated with respect to all airflow, temperature, and water vapor. It was also found that models with a simple garment shape produced the same results as models with a complex geometry on a macroscopic scale. Models with different regions and smaller air gaps between the clothes and the human body should be confirmed.

1 Introduction

People spend most of their time indoors. Therefore, the design of indoor environments is an important research topic. In recent years, computational fluid dynamics (CFD) simulations have been widely recognized as a powerful tool for evaluating the heterogeneous environment around the human body, even though the human body is an environmental component that generates sensible and latent heat (water vapor). The human body is also treated as an objective function in optimization analyses. Many studies have been conducted on the thermal environment around the human body, airflow, and diffusion of pollutants. ([1-3]) However, most of these studies have either ignored the effect of clothing or treated it as imparting simple resistance to heat and scalar variables. The role of clothing is not only to retain heat and water vapor but also to prevent dermal exposure to toxic substances. In particular, in terms of heat and scalar transport, clothing models are often simpler than thermoregulatory models and physiologically based pharmaco-kinetic model (PBPK) that describe heat and scalar transport inside the human body.

This study has the following objectives: (i) to create a garment model that reproduces detailed geometries and has voids, e.g., air gap for ventilation, applicable to thermoregulation and (ii) to implement a coupled analysis of thermoregulation by garments and the flow, temperature, and moisture transfer around the garment. This paper reports preliminary simulation results for the integrated analysis of CFD and computer simulated person (CSP) with clothing.

2 Methods

2.1 Creating a clothed model

Experimental thermal manikins with clothing were subjected to 3D measurements using a 3D laser scanner. The nude manikin and those with clothing were scanned independently to obtain a detailed geometric structure of the air layer between the skin surface and clothing. Based on these scanned experimental thermal manikins, 3D-garment models that could be incorporated into the human body model, i.e., CSP, were created.

Figure 1 shows the results of the 3D human body models with clothing: (a) naked model, (b) human body with a short sleeve model (t-shirt plus trousers), and (c) human body with a long-sleeve model (long-sleeve shirt plus trousers). To investigate the ventilation characteristics in the ventilation air layer of the garment due to the difference in shape, a garment model with the same shape as the surface of the human body model was also created and used as a simplified clothing model: (d) a human body with a simplified short-sleeve model, and (e) a human body with a simplified long-sleeve model.

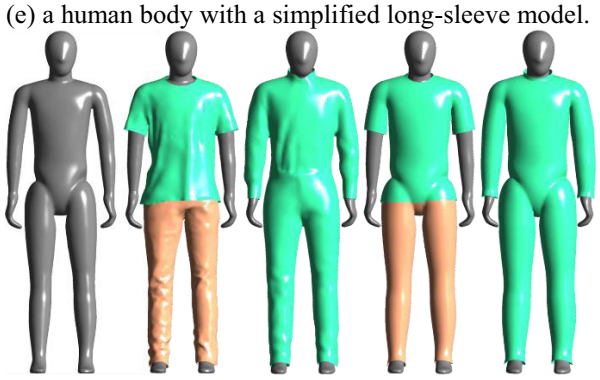

(a) (b) (c) (d) (e)

Figure 1. Numerical human body models; (a) Naked, (b) Short-sleeves (SS), (c) Long-sleeves (LS), (d) Simple-Short-

1 Corresponding author: hyodo.sena.850@s.kyushu-u.ac.jp

sleeves (Simple-SS), and (e) Simple-Long-sleeves (Simple-LS)

In the simplified clothing model, the thickness of the ventilation air layer from the skin to the inner surface of the garment was uniformly created, and the thickness of this layer was the same as the average thickness of the complex geometry made by 3D scanning. In these simplified models, the garment had no thickness as its shape and was used as a hypothetical thickness and physical parameters when calculating the heat and moisture transfer.

The hygrothermal transfer models in garments are shown in Equations (1) and (2):

$$\rho_w \left(\frac{\partial \phi}{\partial \mu} \right) \frac{\partial \mu}{\partial t} = \nabla \left(\lambda'_{Tg} \nabla T + \lambda'_{\mu g} \nabla \mu \right) \tag{1}$$

$$\frac{\partial c \rho_c T}{\partial t} = \nabla \left(\lambda \nabla T \right) + r \rho_w \frac{\partial \phi}{\partial t} \tag{2}$$

where ρ_w is the density of water [kg/m^3], ϕ is the water content [m^3/m^3], μ is the chemical potential of water [J/kg], T is the temperature [K], c is the heat capacity of clothes [J/kg/K], ρ_c is the apparent density of clothes [kg/m^3], λ is the thermal conductivity [W/m/K], λ'_{Tg} is the vapor conductivity for the temperature gradient [kg/m/s/K], $\lambda'_{\mu g}$ is the vapor conductivity for the water chemical potential gradient [kg/m/s/(J/kg)], and r is the latent heat of water [J/kg].

2.2 CFD analysis

To identify the impact of clothing models on the microclimate around the human body and thermal comfort, steady-state flow field, temperature, and moisture transfer analyses were conducted using five types of numerical human bodies (CSP) under naked and clothed conditions. Table 1 shows the boundary conditions of numerical analysis.

Table 1. Analytical and boundary conditions

Turbulence model	SST k-ω model
Inlet	Velocity: 0.1 [m/s] Temperature: 298 [K] Humidity: 9.88 [d/kg'] (RH=50%)
Outlet	Gradient zero
Radiation model	Long-wave Surface-to-Surface model (S2S model)
Emissivity	Skin: 0.98, Clothing: 0.95, Wall: 0.95
Boundary conditions	Velocity: No slip Temperature: (Human body) T_{sk}=36.4-0.054q_{sk} (Wall) Gradient zero Humidity: (Human body) 14.49 [g/kg'] (Wall) Gradient zero

Figure 2 shows the room model containing a CSP with clothing for the integrated CFD analysis. Displacement ventilation type of the supply inlet and exhaust outlet were arranged in the room model. To precisely analyze the air layer between the skin surface and clothing, as well as the temperature, and moisture transfer between the clothing surface and the indoor environment, high-quality meshes at the boundaries and very fine prism mesh layers near the wall surfaces were carefully designed, and the first grid points attached to the wall surfaces were satisfied with the wall unit $y^+ < 1$. The shear stress transport k-ω model was adopted as the turbulence model. Fanger's one-node model was applied as the boundary condition for the skin surface to in order to match the control method of the experimental thermal manikin.

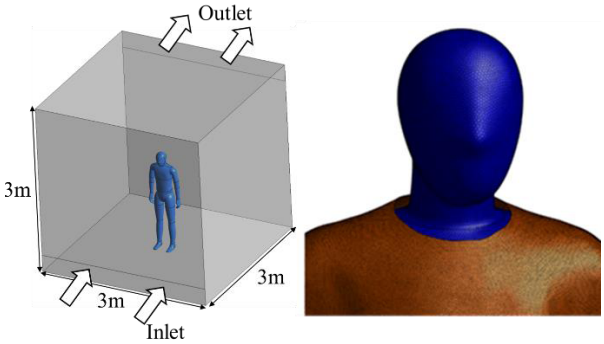

Figure 2. Room model with CSP, boundary mesh of CSP with clothing

3 Results and Discussion

Using the steady CFD results for the flow, temperature, and moisture distributions in and around the CSP, the airflow rate of the air layer between the clothing and the skin surface of CSP, convective heat, and moisture transfer coefficients were quantitatively estimated.

The airflow rate in the ventilation air layer was approximately 80 L/min in models (b), (c), (d), and 135 L/min in model (e). Although the volume of the total air layer was the same in model (c) and model (e), the area of the opening that served as the inlet was twice as large in model (c), which may have had a significant effect on the airflow rate. The airflow rate in the ventilation air gap was estimated to be more than five times higher than that in a previous reported study ([4, 5]), suggesting that the present analysis overestimated the ventilation rate.

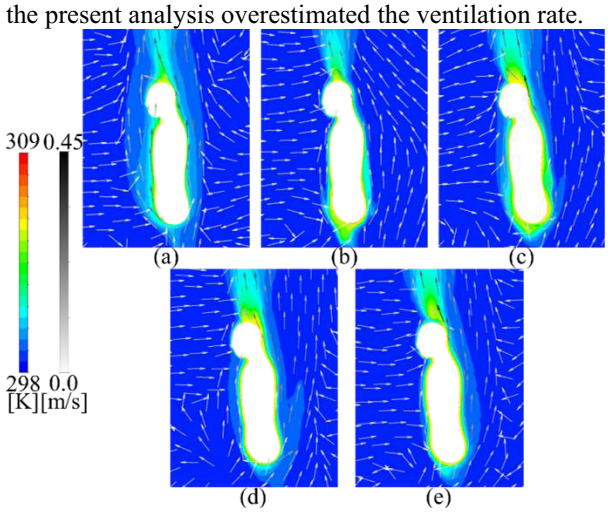

Figure 3. Air Velocity (vector) and Temperature (contour) distributions

Figure 3 shows the generation of a thermal plume around the human body due to metabolic heat generation. The airflow around the human body is affected by the heat generated by the human body and temperature differences, and an upward airflow can be observed

along with the human body. This means that the presence or absence of clothing and the shape of the clothing affect the temperature differences between the skin surface and the reference air temperature, as well as the differences of the characteristics of the surrounding airflow in the vicinity of the human body.

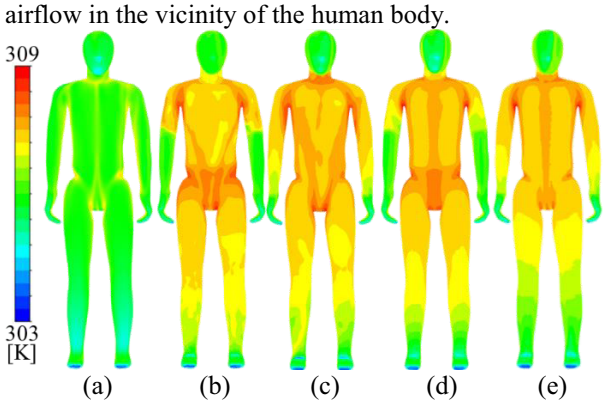

Figure 4. Skin surface temperature distributions for each model

Figure 4 shows the skin surface temperature distribution for each model. In model (a), the naked condition, the skin temperature was significantly lower than the results of other conditions with clothing. The skin temperature in model (a) was 306[K], and the other models in (b), (c), (d), and (e) showed an average skin surface temperature of approximately 307 [K]. Although models (c) and (e) had a larger coverage area of clothing than the others, the area-weighted average temperature of the skin surface was similar in each case. This is because, in the case of models (b) and (d), there is a region where the pants and t-shirt overlap, and the temperature becomes relatively high in this region.

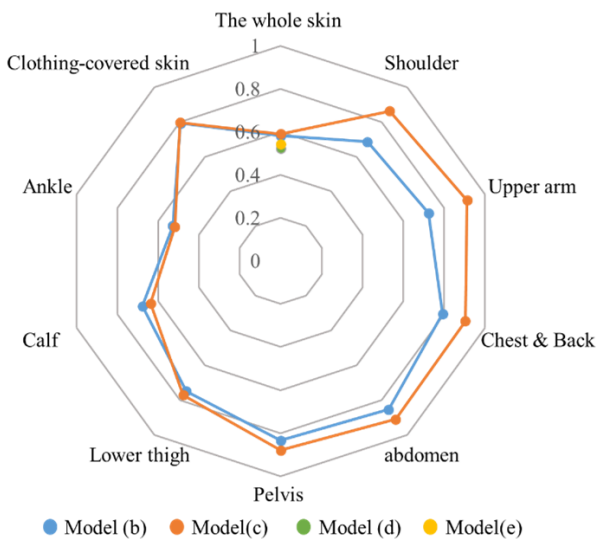

Figure 5. Heat resistance [clo] of models (b), (c), (d) and (e)

Figure 5 shows the heat resistance from the skin surface to the clothing outside the surface, calculated following the conventional calculation procedure for the clo value. For models (b) and (c), the clo values for each segment were calculated in addition to the average values for the entire skin surface. There were no significant differences in whole clo values among the four models. However, when we check the clo values for each segment, it can be observed that there is a significant difference between them. This is because the geometry and ventilation properties of the ventilation air layer of each segment are different.

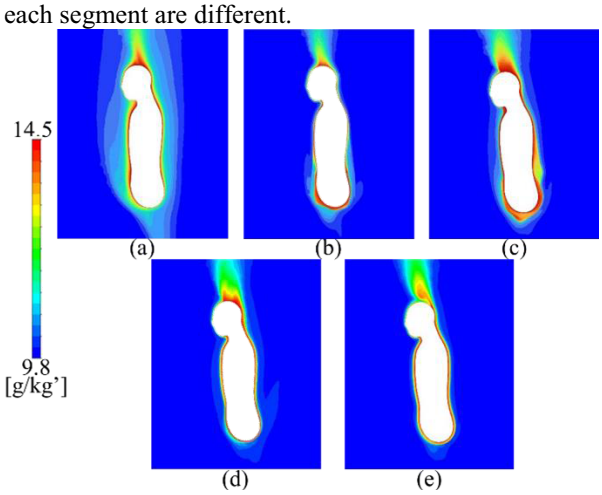

Figure 6. The distribution of vapor concentration in and around the human body

Figure 6 shows that clothing plays a significant role in maintaining water vapor inside the air gap and clothing. The mass flux of water vapor at the skin surface was estimated to be 0.0257 [g/kg'] for model (a), 0.0147 [g/kg'] for model (b), 0.0133 [g/kg'] for model (c), 0.0143 [g/kg'] for model (d), and 0.0155 [g/kg'] for model (e). The water vapor flux of model (e) is relatively larger than that of the other clothing models because of the relatively larger air flow rate in the ventilation air layer.

4 Conclusions

This study reported the development of a realistic clothing model based on 3D scanning technology using real clothes and a comprehensive analysis method, as well as results of the microclimate in and around the human body with clothing.

Steady-state analysis of airflow, temperature, and humidity in a simplified room model was performed, and the results of the analysis of ventilation flow rate in the air gap between clothing and the human body showed that there was a significant difference between the naked and clothed human body models.

When models (d) and (e) were compared with models (b) and (c) in terms of the entire skin surface temperature of the human body, no significant differences were observed from a macroscopic point of view. However, considering the thermo-regulation model with multi-node segmentation for skin surface temperature control, a 3D detailed clothing model that can integrate with CSP and estimate the heat and scalar transport resistance for each body segment may contribute to improving the prediction accuracy of thermal comfort and thermal sensation using CSP.

References

[1] C. Wang, S. Yoo, K. Ito. Advances in Building Energy Research, **14 (4)**, 450-470 (2020)

[2] C. Wang, S. Yoo, S. Tanabe, K. Ito. Energy and Built Environment, **1** 423-431 (2020)
[3] S. Tanabe, E.A. Arens, F.S. Bauman, H. Zhang, T.L. Madsen. ASHRAE Transactions, **100 (1)** 39-48 (1994)
[4] S. Takada, A. Sasaki, R. Kimura. Building and Environment, **99** 210-220 (2016)
[5] R.R. Birnbaum, G.W. Crockford Applied Ergonomics, **9 (4)** 194-200 (1978)